
Fast and Stable Triangular Inversion for Delta-Rule Linear Transformers

Aleksandros Sobczyk * Gioele Gottardo Christos K. Matzoros Mirko De Vita

Filip Skogh

Anastasios Zouzias

Jiawei Zhuang

Computing Systems Lab
Huawei Technologies
Switzerland

Abstract

Linear attention has emerged as a cornerstone for efficient long-context architectures, as evidenced by its integration into state-of-the-art open-source models including Qwen3.5/3.6, Kimi Linear, and RWKV-7. Models that incorporate linear attention layers with the so-called Delta-Rule involve the inversion of triangular matrices as a core sub-routine. This operation often forms a performance bottleneck, and, due to its high-sensitivity to numerical errors, it can significantly deteriorate end-to-end model accuracy if it is not carefully implemented. This work provides a systematic analysis of both direct and iterative triangular inversion algorithms, targeting methods that are rich in matrix products, and, therefore, have the potential to efficiently utilize modern hardware. To that end, our analysis covers a broad spectrum of mathematical and practical aspects, with a heavy focus on numerical stability, computational complexity, and, ultimately, hardware efficiency and practical considerations. We provide a rigorous experimental evaluation to verify these properties in practical scenarios, and in low-precision floating-point representations, highlighting the strengths and limitations of each method. Performance benchmarks on NPUs reveal up to $4.3\times$ speed-up against the state-of-the-art implementations of SGLang for triangular matrix inversion, leading to significant performance improvements on the entire layer level, while maintaining full end-to-end model accuracy.

1 Introduction

The attention mechanism [30] is one of the most important innovations of the last decade in deep learning, and lies at the core of Large Language Models (LLMs). The quadratic time complexity and the linearly growing KV-cache of softmax-attention have become a key bottlenecks for scaling LLMs. Linear attention [16] offers a way to reduce the computational complexity, and many different variants have been developed to close the performance gap between linear and standard attention [5, 17, 21, 37]. Prominent approaches towards this direction include DeltaNets [23, 38] and Gated DeltaNet (GDNs) [36], which introduce decay and gating factors.

In brief, given an input sequence of length L , the corresponding query-key-value matrices $\mathbf{Q}, \mathbf{K}, \mathbf{V} \in \mathbb{R}^{L \times d}$, where d is the head dimension, and a causal mask (lower-triangular) matrix $\mathbf{M} \in \mathbb{R}^{L \times L}$, in

*Contact: aleksandros.sobczyk@h-partners.com gioele.gottardo2@h-partners.com
christos.konstantinos.matzoros@h-partners.com mirko.de.vita@h-partners.com
filip.skogh@h-partners.com anastasios.zouzias@huawei.com zhuangjiawei@huawei.com

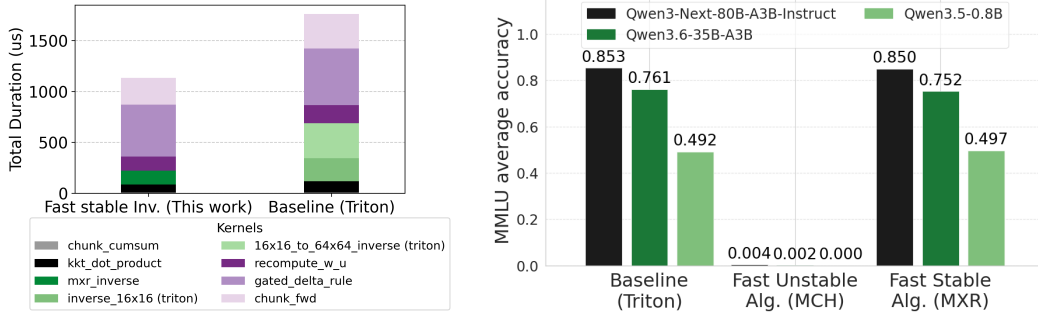


Figure 1: Left: Runtime breakdown of single GDN layer. Right: Accuracy drop in end-to-end benchmark evaluation due to inversion errors accumulation.

its simplest form linear attention can be defined in two equivalent ways:

$$\mathbf{O} = (\mathbf{Q}\mathbf{K}^\top \odot \mathbf{M})\mathbf{V} \quad (\text{matrix form}), \quad (1)$$

$$\mathbf{o}_t = \left(\sum_{i=1}^t \mathbf{v}_i \mathbf{k}_i^\top \right) \mathbf{q}_t = \mathbf{V}_{1:t,:}^\top \cdot \mathbf{K}_{1:t,:} \mathbf{q}_t \quad (\text{linear recurrence}), \quad (2)$$

where \odot denotes element-wise matrix product. The linear recurrence formulation requires significantly less memory than the matrix form, as it only requires a single vector to be stored at any time step. On the other hand, the matrix form lends itself for parallel processing. To achieve the “best of both worlds”, and to optimize the computational capabilities of AI accelerators, a standard technique is to utilize *chunk-wise* parallel processing [14, 38]. In this case, the sequence is partitioned into $\lceil L/C \rceil$ “chunks” of (at most) length C each. In practice, C is typically one of $\{16, 32, 64, 128\}$. Let us denote the corresponding “chunks” of the matrix \mathbf{K} as $\mathbf{K}_{[k]} := \mathbf{K}_{kC:(k+1)C,:} \in \mathbb{R}^{C \times d}$. After several non-trivial mathematical re-formulations (see e.g. [36]), the final output updates within each chunk require the computation of the inverse of a *unit-diagonal lower triangular matrix* \mathbf{A} of size $C \times C$, which has the form:

$$\mathbf{A}_{[k]}^{-1} = \left(\mathbf{I} - \phi(\mathbf{K}_{[k]}, \mathbf{K}_{[k]}^\top) \odot \mathbf{L}^- \right)^{-1}, \quad \mathbf{L}_{i,j}^- := \begin{cases} 0, & \text{if } i \leq j, \\ 1, & \text{otherwise,} \end{cases} \quad (3)$$

where $\phi(\cdot, \cdot) \in \mathbb{R}^{C \times C}$ is a function that depends on the specific model architecture, typically involving element-wise functions of the elements of \mathbf{K} , such as scaling or exponentiation, \mathbf{I} is the identity matrix, and \mathbf{L}^- is a strictly lower triangular all-ones (mask) matrix of size C . We provide a description of the different $\phi(\cdot, \cdot)$ functions that are used by various models in Table 1.

Table 1: Examples of functions $\phi(\cdot, \cdot)$ in existing models.

Model	$\phi(\cdot, \cdot)$
DeltaNet [23]	$\text{diag}(\beta) \cdot \mathbf{K}\mathbf{K}^\top$
DeltaFormer [35]	$\exp(\mathbf{W}\mathbf{K}^\top)$
GDN [36]	$\mathbf{K}\mathbf{K}^\top \odot \mathcal{A}$
Comba [13]	$\mathbf{K}\mathbf{K}^\top \odot \mathcal{A}^{i-1/j}$
KDA [17]	$(\mathbf{K} \odot \mathbf{\Gamma})(\mathbf{K} \odot \mathbf{\Gamma})^\top$

Table 2: Summary of triangular inversion methods.

Method (Acronym)	Type	Stability	# MatMuls	Refs.
Vector Col. Sweep (VCS)	Direct	stable (Lem. 3.1)	-	[8, 22]
Matrix Col. Sweep (MCS)	Direct	stable (Lem. 3.1)	$O(n)$	[8, 22]
Bunch-Hopcroft (MBH)	Direct	log-stable	$\approx 2 \log(n)$	[1, 6]
Cayley-Hamilton (MCH)	Direct	unstable	$2 \lceil \log(\frac{n}{2}) \rceil$	[4]
Mixed Recursion (MXR)	Direct	log-stable	$\approx 2 \log(n)$	Sec. 3.4
Newton-Schulz (NS)	Iterative	stable (conjectured)	$2 \times N_{\text{iter}}$	[19, 24]
Iterative Refinement (IR)	Iterative	stable (per iter)	$2 \times N_{\text{iter}}$	[12]

1.1 Motivation and Contributions

In existing model implementations, the actual inversion of the individual chunks can quickly become a performance bottleneck. For example, in Figure 1 (Left) it is shown that the triangular inversion part can take up to $\sim 40\%$ of the total layer device-runtime.

Alternative approaches for hardware-aware algorithms have been proposed [41] to better utilize matrix cores in AI accelerators and to surpass the performance bottlenecks. However, matrix cores are

usually optimized for low-precision (half) arithmetic, and hence if these hardware-aware algorithms are not designed carefully, the errors introduced due to low-precision floating point arithmetic can easily lead to catastrophic accumulation of errors, often returning completely wrong, or even "NaN" solutions. This is clearly illustrated in Figure 1 (Right), where we show how an unstable inversion method drastically reduces the reasoning capabilities of Qwen3.6, dropping the accuracy on MMLU from 75.6% to 0.2%! Evidently, model accuracy is highly correlated to the accuracy of the underlying inversion algorithm.

This is of course not surprising. Inverting triangular matrices, or, even more importantly,² solving triangular systems of linear equations, is a very thoroughly studied problem in numerical analysis, dating all the way back to the early works of Wilkinson [34]. One of the main reasons is that triangular factorizations (LU, Cholesky, QR, etc) established themselves early-on as the “gold standard” procedure to solve general (dense) linear systems of equations. As such, the stability properties and computational complexity are quite well-understood, and algorithm implementations should always take them into consideration and carefully handle numerical errors.

The aforementioned observations motivated us to revisit the rich bibliography on triangular matrix inversion algorithms, in the context of Linear Transformers. We focus on deriving algorithms based on the following guidelines:

Matrix products and hardware efficiency: In order to take advantage of matrix cores in modern AI accelerators, the underlying inversion algorithms should extensively use matrix products.

Numerical stability: Fast algorithms are not useful if they return wrong results. To that end, numerical stability analysis is mandatory to ensure high-accuracy and meaningful results in real-applications.

Focus on Linear Attention: The specific properties of the matrices arising in Delta-Rule Linear Transformers should be exploited as much as possible to achieve the best performance, both from the mathematical analysis perspective, as well as practical performance.

Our main contribution is the thorough analysis of several types of direct and iterative triangular inversion algorithms, based on the aforementioned guidelines. A summary of the methods studied here and their properties is provided in Table 2.

By dedicating the analysis to the underlying types of matrices, we provide some novel mathematical properties that are also useful for practical applications. Stability properties are thoroughly tested experimentally for all algorithms, in three different precisions: float32, float16, and bfloat16. Interestingly, we show that even *abysmally unstable* algorithms (Alg. 5, MCH), if used carefully, can be efficiently exploited as sub-routines inside very fast and stable algorithms (Alg. 2, MXR). In terms of performance, the latter approach achieved up to 4.3x speedup on NPUs compared to the current state-of-the-art implementations for triangular inversion in SGLang. Links to the public repositories that contain the source code are provided in Appendix A

Acknowledgements

We thank Efstratios Gallopoulos for helpful literature recommendations, and for suggesting the term “abominable” to characterize the condition number of random triangular matrices.

2 Preliminaries

2.1 Numerical stability

Fast algorithms are not useful if the returned results are not accurate. In this section, we recall a notion of numerical stability for matrix inversion (see e.g. [7, 12]), which allows us to argue about the robustness of different algorithms against numerical errors. It is especially important in low-precision scenarios, which are becoming more and more prominent in AI workloads. We assume a standard floating-point model of computation with t bits for the significand, p bits for the exponent, and one bit for the sign. The machine precision is equal to $\mathbf{u} := 2^{-t}$. (see Appendix B for a detailed description).

²Folklore states that, for many numerical analysts, inverting a matrix is considered a sin, since, in many cases, all that one needs is to solve a linear systems of equations, rather than computing the entire inverse.

Definition 2.1. Let \mathbf{A} be an invertible $n \times n$ triangular matrix. An algorithm A which computes an approximate inverse $\tilde{\mathbf{A}}^{-1}$ is said to be f -stable if:

$$\left\| \mathbf{A}^{-1} - \tilde{\mathbf{A}}^{-1} \right\|_2 \leq c_1 \cdot n^{c_2} \cdot \kappa_2^f(\mathbf{A}) \cdot \mathbf{u} \cdot \left\| \mathbf{A}^{-1} \right\|_2,$$

where c_1 and c_2 are global constants (independent of the matrix size n), and $\kappa_2(\mathbf{A}) = \left\| \mathbf{A} \right\|_2 \left\| \mathbf{A}^{-1} \right\|_2 \geq 1$ is the spectral-norm condition number of \mathbf{A} .

In the above definition, f can be a constant, or a function of n . For more details and different notions of numerical stability we refer to standard textbooks [8, 9, 12] and references therein. Throughout the paper, we might refer to $O(1)$ -stable algorithms as “fully-stable” or simply “stable”, and to $\text{polylog}(n)$ -stable algorithms as “logarithmically-stable” or “log-stable”, as coined in [6].

2.2 Triangular matrices and their condition number

One of the “challenging”, and intriguing, facts about triangular matrices in general, is that they can easily have an abominable condition number: Viswanath and Trefethen proved that the matrix $\mathbf{I} + \text{strict_tril}(\mathbf{G})$, where $\mathbf{G}_{i,j} \sim \mathcal{N}(0, 1)$, almost surely has an *exponentially growing* condition number [31]. Since the floating point errors in matrix inversion depend on the condition number of the input, this fact seems very discouraging for inverting matrices in linear transformers, since they are also triangular with unit diagonal elements. Luckily, this is not the case. One of the key observations for our analysis is that matrices of the form of Eq. (3) are actually *well-conditioned*. This is necessary to justify the use of low-precision compute units for such operations, and it also reveals why such implementations have been working well in practice to-date. In [15], it was proved that the elements of the inverse of a DeltaNet matrix are always in $[-1, 1]$. The following implication is immediate (a simple proof can be found in Appendix C.1).

Corollary 2.1. *The condition number of an $n \times n$ DeltaNet matrix \mathbf{A} is at most n^2 .*

Note that the scaling $\phi(\cdot, \cdot)$ that takes place in Eq. (3) typically reduces the magnitude of the off-diagonal elements, in which case it is expected to further reduce the condition number as the matrix becomes more-and-more diagonally dominant. In that respect, these types of matrices are much better conditioned than random triangular matrices, which is promising towards exploiting low-precision hardware and fast (potentially less stable) algorithms.

Algorithm 1 MCS(\mathbf{L}, n): 1: $\mathbf{L} \leftarrow 2\mathbf{I} - \mathbf{L}$ 2: $\mathbf{X} \leftarrow \mathbf{I}$ 3: for $k = n - 1$ down to 0 : 4: $\mathbf{M} \leftarrow \mathbf{I} + \mathbf{L}[:, k] \cdot \mathbf{e}_k^\top$ 5: $\mathbf{X} \leftarrow \mathbf{M} \cdot \mathbf{X}$ 6: return \mathbf{X}	Algorithm 2 MXR($\mathbf{L}, n, b_0, r = 0$): 1: $\mathbf{D} \leftarrow b_0 \times b_0$ diagonal blocks of \mathbf{L} 2: $\mathbf{Y} \leftarrow \text{MCH}(\mathbf{D}, b_0)$ 3: for $i = 1, \dots, r$: 4: $\mathbf{Y} \leftarrow \text{IR}(\mathbf{Y}, \mathbf{L})$ ▷ Alg. 6 5: $\mathbf{X} \leftarrow \text{MBH}(\mathbf{L}, n, \mathbf{Y}, b_0)$ ▷ Alg. 4 6: return \mathbf{X}	Algorithm 3 NS($\mathbf{L}, n, m, \mathbf{X}_0$): 1: $\mathbf{A} \leftarrow \mathbf{I} + \mathbf{L}$ 2: $\mathbf{X} \leftarrow \mathbf{X}_0$ 3: for $k = 0, \dots, m - 1$: 4: $\mathbf{Y} \leftarrow \mathbf{A} \cdot \mathbf{X}$ 5: $\mathbf{X} \leftarrow 2\mathbf{X} - \mathbf{X} \cdot \mathbf{Y}$ 6: return \mathbf{X}
Algorithm 4 MBH($\mathbf{L}, n, \mathbf{X}_0 = \mathbf{I}, b_0 = 1$): 1: $\mathbf{X} \leftarrow \mathbf{X}_0$ 2: for $b = b_0, 2b_0, 4b_0, \dots, n$: 3: $\mathbf{D}_e \leftarrow$ even $b \times b$ diagonal blocks of \mathbf{X} 4: $\mathbf{D}_o \leftarrow$ odd $b \times b$ diagonal blocks of \mathbf{X} 5: $\mathbf{X} \leftarrow \mathbf{D}_e + \mathbf{D}_o - \mathbf{D}_o \cdot \mathbf{L} \cdot \mathbf{D}_e$ 6: return \mathbf{X}	Algorithm 5 MCH(\mathbf{L}, n): 1: $\mathbf{X} \leftarrow \mathbf{I} - \mathbf{L}$ 2: $\mathbf{Y} \leftarrow \mathbf{L}$ 3: for $k = 1, 2, \dots, \log(\frac{n}{2})$: 4: $\mathbf{Y} \leftarrow \mathbf{Y} \cdot \mathbf{Y}$ 5: $\mathbf{X} \leftarrow \mathbf{X} + \mathbf{X} \cdot \mathbf{Y}$ 6: return \mathbf{X}	Algorithm 6 IR(\mathbf{Y}, \mathbf{L}): 1: $\mathbf{A} \leftarrow \mathbf{I} - \mathbf{L}$ 2: $\mathbf{R} \leftarrow \mathbf{I} - \mathbf{Y}\mathbf{A}$ 3: $\mathbf{X} \leftarrow \mathbf{Y} + \mathbf{R}\mathbf{Y}$ 4: return \mathbf{X}

3 Analysis of methods

In this section, we provide the analysis of the main triangular inverse methods considered here, in terms of their stability properties and their computational complexity. Complexity is mainly focused on matrix products, which is also in-line with recent proposals on models of computation that focus on modern AI accelerators [2, 3, 27, 42]. A fine-grained “bit complexity” analysis can be inferred by the floating point precision bounds. Algorithms 1-6 provide a high-level description of the methods.

3.1 Vectorized and matrix product-based column-sweep (VCS and MCS)

The first algorithm that we discuss is the one proposed by Sameh and Brent [22], which, to our knowledge, was the first parallel algorithm to solve triangular systems with logarithmic depth. It is often referred to as the *column-sweep* method, and it can be implemented in a vectorized form, or in a matrix product-based formulation (see also [8]).

Lemma 3.1. *Column-sweep is numerically-stable, as per Definition 2.1. For well-conditioned matrices (e.g. DeltaNet) that satisfy Corollary 2.1, $t = \log(1/\epsilon) + O(\log(n))$ bits of accuracy are sufficient so that the returned solution $\tilde{\mathbf{A}}^{-1}$ satisfies $\|\tilde{\mathbf{A}}^{-1} - \mathbf{A}^{-1}\|_2 \leq \epsilon \|\mathbf{A}\|_2^{-1}$, for any $\epsilon \in (0, 1)$.*

Proof. The proof can be found in Appendix C.2. □

The corresponding matrix product-based formulation is described in Algorithm 1. In general, the MCS algorithm below generates the matrices $\mathbf{M}_{n-1}\mathbf{M}_{n-2}\dots\mathbf{M}_1$ and performs the chained matrix products. One drawback of the MCS method is that, for matrix size n , it requires $n - 1$ matrix products. In terms of operations, the complexity of these two algorithms is as follows:

Complexity (VCS): $O(n^2)$ **vector ops** of length $n, n - 1, n - 2, \dots, 2, 1$.

Complexity (MCS): $n - 1$ **matmuls** of size $n \times n$, $O(n)$ **vector ops** of length $O(n)$.

3.2 Inverse via characteristic polynomial (MCH)

The main drawback of the coulumn-sweep algorithm is that it executes $O(n)$ square matrix products of size n . The authors of [41] highlight that an alternative algorithm can be considered for such cases, which reduces inverse computation to $O(\log(n))$ matrix products. It can be straightforwardly derived from *Cayley–Hamilton theorem*, by noting that all eigenvalues are equal to one, and therefore the characteristic polynomial can be derived analytically. The inverse in this case is given by:

$$(\mathbf{I} + \mathbf{L})^{-1} = \mathbf{I} - \mathbf{L} + \mathbf{L}^2 - \mathbf{L}^3 + \dots + (-1)^n \mathbf{L}^n, \quad (4)$$

where \mathbf{L} is an arbitrary strict triangular square matrix of size n , and it can be quickly computed via repeated squaring: we first set $\mathbf{X} \leftarrow \mathbf{I} - \mathbf{L}$ and $\mathbf{Y} \leftarrow \mathbf{L}$, and, thereafter, for $i = 1, \dots, \lfloor \log(n) \rfloor - 1$, the algorithm updates first $\mathbf{Y} \leftarrow \mathbf{Y} \cdot \mathbf{Y}$, and then $\mathbf{X} \leftarrow \mathbf{X} + \mathbf{X} \cdot \mathbf{Y}$. It finally returns the last \mathbf{X} . An algorithmic description is listed in Algorithm 5.

Complexity (MCH): $\approx 2 \log(n)$ square matrix products of size n .

In terms of stability, this algorithm and other ones related to the characteristic polynomial are known to have terrible numerical properties (see e.g. the discussion in [4]). The main issues arise due to the rapid growth of intermediate values caused by the repeated squaring. Consider for example the matrix $\mathbf{A} = \mathbf{I} + \mathbf{L}^-$ where \mathbf{L}^- is the strict lower triangular matrix with all entries equal to -1 . After $\log(k)$ iterations of MCH, the elements of the matrix $\mathbf{Y}_k = (\mathbf{L}^-)^k$ can be derived analytically: $(\mathbf{L}^-)^k_{i,j} = \binom{i-j-1}{k-1}$. Specifically, the element $(\mathbf{L}^-)^{n/2}_{n,1} = \binom{n-2}{n/2-1}$, grows approximately as $\sim 2^n / \sqrt{n}$, up to constant factors. This can easily lead to overflow, especially in low-precision formats. However, as long as the algorithm is restricted to very small (constant-sized) matrices, the numerical errors can be maintained to an acceptable level. While this algorithm should be generally avoided, it can be used (carefully) as a subroutine for handling the inverses of small diagonal blocks during the execution of more stable algorithms.

3.3 A log-stable matrix recursive algorithm (MBH)

In this section, we revisit a recursive triangular inversion algorithm, which we call MBH, since (to our knowledge) the first analysis is due to Bunch and Hopcroft [1]. In [6] it was proved that the algorithm is polylog(n)-stable. The algorithm is based on the following observation:

$$\mathbf{A}^{-1} = \begin{pmatrix} \mathbf{A}_{11} & \mathbf{A}_{12} \\ 0 & \mathbf{A}_{22} \end{pmatrix}^{-1} = \begin{pmatrix} \mathbf{A}_{11}^{-1} & -\mathbf{A}_{11}^{-1}\mathbf{A}_{12}\mathbf{A}_{22}^{-1} \\ 0 & \mathbf{A}_{22}^{-1} \end{pmatrix}. \quad (5)$$

where \mathbf{A}_{11} and \mathbf{A}_{22} are square matrices. At each step, it involves computing the inverses of two matrices of half the size, and two matrix products of half the size. In practice, when the individual

sub-blocks become very small, it can become a waste of resources to launch a separate matrix product for each tiny block. Instead, it is preferable to use an “unrolled” recursion, in order to group together small matrix products that occur at the lowest levels of the recursion. The stability analysis of [6], together with Corollary 2.1, implies a bound on the number of precision bits.

Proposition 3.1. *Fix $\epsilon \in (0, 1)$. It is sufficient to use $t = \log(1/\epsilon) + O(\log^c(n))$ bits of precision to invert a well-conditioned matrix \mathbf{A} that satisfies Corollary 2.1 (e.g. DeltaNet), using Alg. 4, such that the returned solution $\tilde{\mathbf{A}}^{-1}$ satisfies $\|\tilde{\mathbf{A}}^{-1} - \mathbf{A}^{-1}\|_2 \leq \epsilon \|\mathbf{A}^{-1}\|_2$.*

Complexity (MBH): $\approx 2 \log(n)$ matrix products of size $n \times n$ (proof in Appendix C.3).

3.4 A mixed recursive algorithm (MXR)

One issue of the recursive algorithm of the previous section is that, for “tiny” block-sizes, it needs to execute two full $n \times n$ matrix multiplication per iteration, while most of the elements in these cases are almost zero, since the matrices are almost diagonal. To overcome this for practical purposes, we propose to use the unstable algorithm of Section 3.2 only for a few initial iterations, e.g., for block-sizes up to 16×16 , in order to compute the small diagonal inverses as a starting point, and then continue the log-stable iteration for the later steps. This increases the hardware utilization, and, since the unstable algorithm is only executed for constant-sized blocks, the full algorithm in its entirety remains logarithmically stable (albeit, the “constant errors” might be large, and should still be treated with care). An example of this approach, which we later show to be extremely efficient in practice, is outlined below (see also Algorithm 2):

1. Use the algorithm of Section 3.2 in order to compute the small inverses of the diagonal blocks of \mathbf{A} , where each block has size $C \times C$ for some constant C (e.g., $C \in \{16, 32\}$).
2. Use the unrolled recursive algorithm of Section 3.3 to compute the final inverse.

The stability properties of Algorithm 2 are summarized in Theorem 3.1.

Theorem 3.1. *Algorithm 2 is polylog(n)-stable for all input matrices \mathbf{L} with $\|\mathbf{L}\|_2 = \text{poly}(n)$.*

Proof. When $\|\mathbf{L}\|_2 = \text{poly}(n)$, Lemma C.2 in the appendix implies that the MCH algorithm, which inverts the small diagonal blocks in the first phase, requires at most $\log(1/\epsilon) + \text{polylog}(n)$ bits of precision to return ϵ -approximate block-inverses, i.e., the first phase is polylog(n)-stable. In the second phase, Algorithm 4 takes as input those initial block-inverses to compute the entire inverse, and from [6] we know that this second phase is also polylog(n)-stable. \square

Complexity (MXR): $\approx 2 \log(n)$ matrix products of size $n \times n$.

3.5 Iterative inversion with Newton-Schulz

All aforementioned algorithms so far are *direct*, in a sense that, in exact arithmetic, they return the exact inverse after a finite number of steps. In this section we revisit the Newton-Schulz iteration [24], which, as Higham highlights in [12], “...is attractive because it involves only matrix multiplication”. Given a square matrix \mathbf{A} , and an initial guess \mathbf{X}_0 for the inverse of \mathbf{A} , the method iteratively updates:

$$\mathbf{X}_{k+1} \leftarrow \mathbf{X}_k(2\mathbf{I} - \mathbf{A}\mathbf{X}_k), \quad k = 0, 1, 2, \dots \quad (6)$$

This iteration has been studied in depth for computing the inverse and/or pseudo-inverse of general matrices [19, 20, 28, 39], but we are not aware of a dedicated analysis for unit-diagonal triangular matrices. Nevertheless, we can obtain quite strong convergence and stability guarantees from existing analyses. In [19], Pan and Reif provide explicit bounds on the convergence and number of iterations.

With a straightforward error analysis, one can show that a single iteration of Newton-Schulz is numerically stable. However, carrying over the analysis to multiple iterations to achieve end-to-end numerical stability for the inverse, as in Definition 2.1, is quite tedious. At this point we can refer to the recent and very rigorous analysis of Shah [26], who showed end-to-end stability guarantees of the Newton-Schulz iteration for the sign function, and proved that, indeed, the method is stable for that task. Given the existing analyses, there is no reason to suspect that Eq. (6) is unstable. However, to our knowledge, a formal proof remains an interesting open question. The next proposition directly follows from the analysis in [19] and the stability assumption. The proof is located in Appendix C.4

Proposition 3.2 (Follows from [19]). *Fix $\epsilon > 0$. Assume that the Newton-Schulz method is stable, in a sense that, after k iterations, the returned matrix $\tilde{\mathbf{A}}^{-1}$ satisfies $\|\hat{\mathbf{A}}^{-1} - \tilde{\mathbf{A}}^{-1}\|_2 \leq \mathbf{u} \cdot (n \cdot \kappa(\mathbf{A}))^{O(1)} \cdot \|\mathbf{A}^{-1}\|_2$, where $\hat{\mathbf{A}}^{-1}$ is the true matrix after k iterations in exact arithmetic. Then, for $\text{poly}(n)$ -conditioned triangular matrices, after $O(\log(n))$ iterations $\tilde{\mathbf{A}}^{-1}$ satisfies $\|\tilde{\mathbf{A}}^{-1} - \mathbf{A}^{-1}\|_2 \leq \epsilon \|\mathbf{A}^{-1}\|_2$ using $t = \log(1/\epsilon) + O(\log(n))$ bits of precision, using $\mathbf{X}_0 = \mathbf{I}/n^{O(1)}$ as an initial guess.*

Complexity (NS): $2 \times N_{iter}$ matrix products of size $n \times n$ (typically $N_{iter} \approx 2 \log(n)$).

3.6 Iterative refinement

A standard technique to improve the accuracy of numerical algorithms for solving linear systems of equations (especially in floating point arithmetic) is iterative refinement [11, 18, 33]. In the context of this work, we use the following iterative scheme. If $\tilde{\mathbf{A}}_0^{-1}$ is the approximate inverse returned by an algorithm, then for $k = 0, 1, \dots$ we iteratively update:

$$(i) \mathbf{R}_k \leftarrow \mathbf{I} - \tilde{\mathbf{A}}_k^{-1} \mathbf{A}, \quad (ii) \tilde{\mathbf{A}}_{k+1}^{-1} \leftarrow \tilde{\mathbf{A}}_k^{-1} + \mathbf{R}_k \tilde{\mathbf{A}}_k^{-1}. \quad (7)$$

As it is shown later in the numerical experiments, this simple iterative scheme, which involves only two matrix products per iteration, can significantly increase the final accuracy in some cases, even with a single iteration.

4 Evaluating the numerical accuracy of the methods

In this section we evaluate experimentally the numerical accuracy of all the aforementioned methods.

4.1 Accuracy of the computed inverse

We first assess the accuracy of each method in terms of the posterior errors of the returned inverse compared to the true inverse of the input matrix. For the experimental results illustrated in Figure 2, the input matrix is equal to $\mathbf{A} = \mathbf{I} + \mathbf{L}$, where $\mathbf{L} := \text{strict_tril}(\mathbf{K}\mathbf{K}^\top)$, and the rows of \mathbf{K} are samples independently from the unit sphere, resembling standard DeltaNet matrices.

The “true inverse” \mathbf{A}^{-1} is obtained computationally by calling the inverse functions provided by PyTorch in double-precision, which internally calls BLAS/LAPACK routines that are highly accurate. To have a broad overview, we measure three different types of forward errors:

$$\text{Max abs.: } \max_{i,j} |\mathbf{A}_{i,j}^{-1} - \tilde{\mathbf{A}}_{i,j}^{-1}|, \quad \text{Max rel.: } \max_{i,j \leq i} \frac{|\mathbf{A}_{i,j}^{-1} - \tilde{\mathbf{A}}_{i,j}^{-1}|}{|\mathbf{A}_{i,j}^{-1}|}, \quad \text{Frob.-norm relative: } \frac{\|\mathbf{A}^{-1} - \tilde{\mathbf{A}}^{-1}\|_F}{\|\mathbf{A}^{-1}\|_F}.$$

We report results for three different types of numerical precision for the inputs: float16, bfloat16, and float32. Internally in the algorithms, matrix products are always executed in float32 precision, even if they receive the input matrices in lower precision; this is standard in modern hardware, since every matrix product might need more bits to store the final result. In single precision, all methods except MCH and MXR return very accurate results, where the relative errors are close to machine precision. MXR (without refinement) achieves about two to three fewer digits of accuracy than the other methods on average, but this is remediated with a single step of iterative refinement. The unstable algorithm, MCH, returns completely wrong results for sizes 64 and 128, but the errors are within acceptable range for size 16, and barely acceptable for size 32.

In the half-precision case, float16, the errors of all methods increase substantially. The errors are no longer within the ideal machine precision error range, but they are still within an acceptable threshold, achieving about three-to-four digits of accuracy on average. The unstable algorithm returns NaN values for all sizes above 16, while, again, MXR achieves decent accuracy, which is on-par with the other methods after a single step of iterative refinement.

The bfloat16 format slightly “improves” the accuracy of the unstable MCH algorithm: the returned values are no longer NaN, which is expected since bfloat16 has a larger exponent range than float16, and can help with extremely large values. However, the errors of MCH remain unacceptably large, and all the returned digits are completely wrong. At the same time, all other methods return higher errors

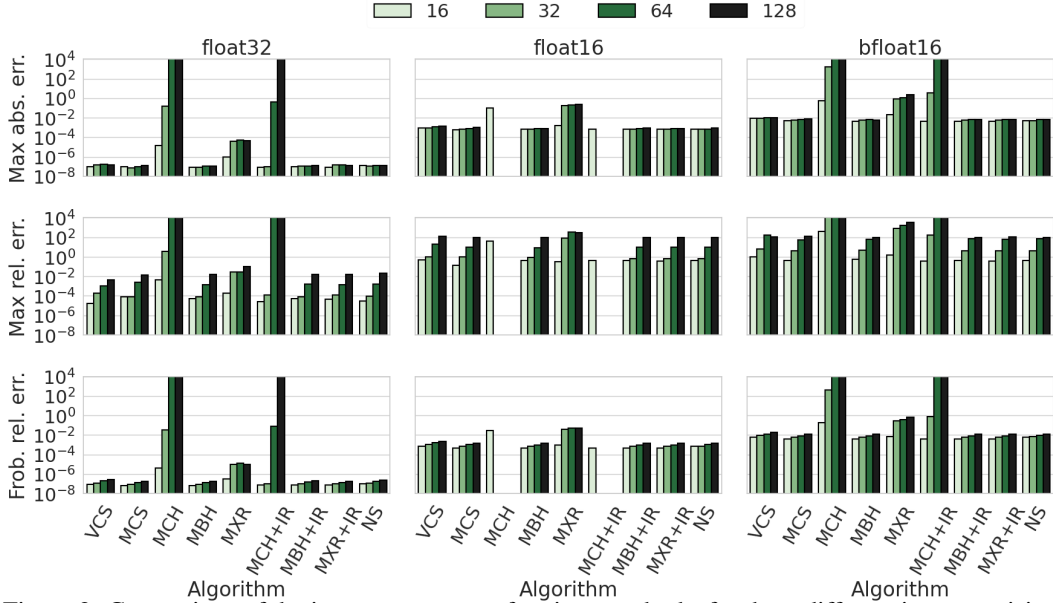


Figure 2: Comparison of the inverse accuracy of various methods, for three different input precision formats, and four matrix sizes.

in bfloat16 than in float16, since bfloat16 uses fewer bits for the mantissa. With these observations, float16 should be preferred against bfloat16 for inverting triangular matrices in linear transformers architectures.

4.2 The effect of numerical accuracy in end-to-end benchmarks

As already indicated in Fig. 1 (right), an unstable algorithm such as Alg. 5 can easily collapse the model accuracy to zero. In the Appendix (Fig. 7) we show that all the stable algorithms, including Alg. 2 (MXR) which uses Alg. 5 as a subroutine, maintain end-to-end accuracy for three different models. The end-to-end accuracy is obtained by modifying the current implementation of the inverse on SGLang [40] to use our algorithms, and then by running the MMLU [10] benchmark over 10 different subjects (for more details on the MMLU benchmark we refer to Appendix D.3). The optimized kernels of SGLang that we use as baseline can be found online [25] and such baseline is labeled in Fig. 1 (right) as “Triton”. We keep the same naming throughout the whole paper.

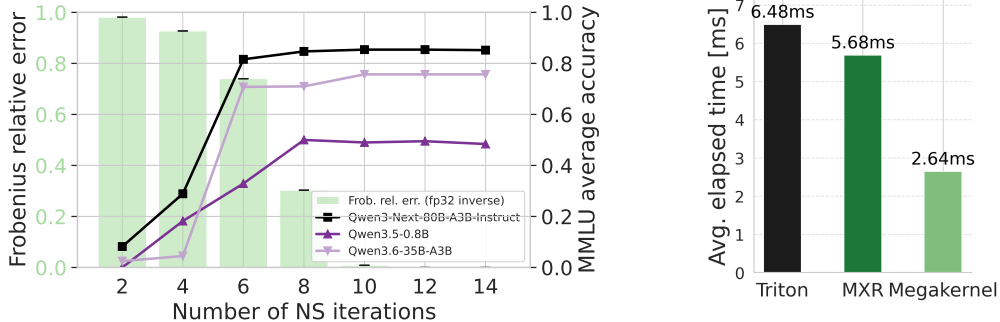


Figure 3: Number of Newton-Schulz iterations (x-axis) versus matrix inversion error using fp32 (left y-axis) and MMLU average accuracy (right y-axis). Chunk size $C = 64$.

Figure 4: GDN layer run on device using Qwen3.5-0.8B tensors as input ($B=8$, $N=16$, $S=1024$, $C = 64$ or $C = 128$)

We next investigate numerical accuracy in more detail by analyzing how errors in computing the triangular inverse affect end-to-end model performance. We employ the Newton–Schulz method and evaluate it at different iteration counts. For each checkpoint, we measure the relative error with

respect to the double-precision inverse computed using NumPy, as well as the average accuracy of several models on MMLU.

Interestingly, as seen in Fig. 3, even after only six iterations, the model already starts to perform relatively well, with 81.6% accuracy for Qwen3-Next-80B-A3B-Instruct. While this is an impressive result considering the relative errors, the accuracy drops are still significant: 4.9% (Qwen3.6-35B-A3B), 16.6% (Qwen3.5-0.8B), and 3.8% (Qwen3-Next-80B-A3B-Instruct) compared to the 12-iteration setting, which ensures numerical stability. We further observe that increasing the number of iterations beyond the optimal value (e.g., 14 iterations) does not have any noticeable effect on end-to-end performance.

5 Performance evaluation and optimization strategies

In this section we report some insights on the performance of the studied algorithms on NPUs, which have recently received significant attention especially for inference tasks. The goal is to understand to which extent the proposed algorithms can efficiently utilize the underlying hardware of modern AI accelerators, and how competitive they are with well-established implementations (Triton, TileLang [32]) on major LLM-serving frameworks.

The NPU devices used in our experimentation contain 48 SIMD units and 24 matrix multiplication cores capable of performing square matrix multiplication of size up to 128. The theoretical memory bandwidth is 1.2 TB/s. The host is an ARM-based CPU with 48 cores. Major LLM serving frameworks, in particular, SGLang and vLLM, officially support NPUs and provide optimized inverse primitives that we use as baselines.

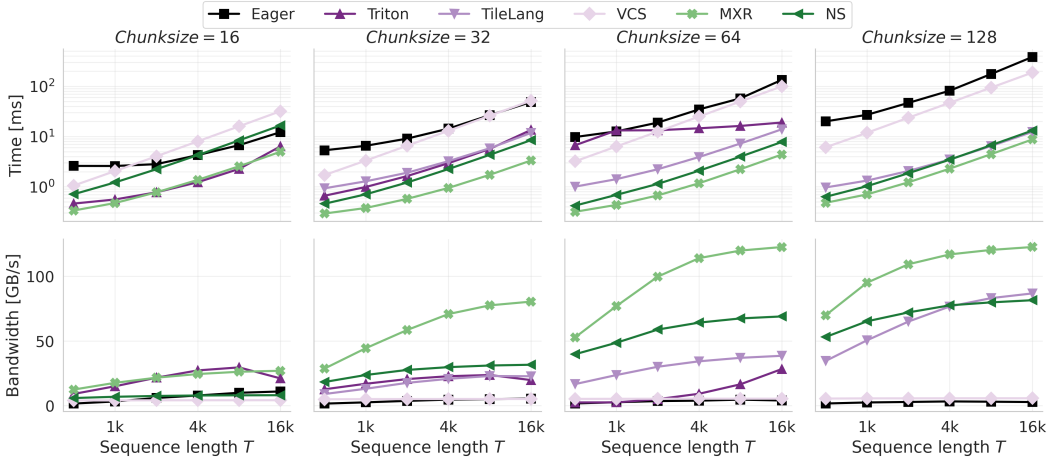


Figure 5: Kernel evaluation of different inverse algorithms. $B = 32$, $N = 4$ and varying sequence length up to $16K$.

5.1 Scalability of individual inverse kernels

At the kernel level, we measure the execution time of the algorithms in isolation. We run 5 warm-up iterations followed by 20 measured iterations, and clear the data cache before each iteration. We set batch size 32, 4 attention heads, and varying sequence length up to $16K$. In Fig. 5, we compare our algorithms against three baselines. The Pytorch Eager reference is a basic python implementation based on the column-sweep algorithm. The Triton implementation is the official implementation for SGLang on NPUs [25] and uses a variation of the BCH algorithm. The Tilelang implementation is another kernel that is provided by the Tilelang framework for NPUs [29] as an example of optimized algorithm. They also used a similar approach to Triton’s, but in a different framework, and by materializing some dimensions of the input.

Our best algorithm, MXR, achieves up to $4.3\times$ speedup over the official implementation and a $3\times$ speedup over TileLang. This confirms that MXR is the best among the proposed candidates as a fast and stable triangular inverse algorithm for GDNs on NPUs.

5.2 Full-layer performance comparison

To see how our kernels performs at the layer level we embed our best performing kernel, MXR, into the GDN layer implemented in [25]. By doing so we improve the layer performance by $1.14\times$ compared to the existing implementation, (See Fig. 4). As it is well-known, however, improvements at the kernel level can easily get “absorbed” in end-to-end benchmarks by other, unoptimized kernels, due to Amdahl’s law. To that end, we further improved the GDN layer by developing our own GDN “mega-kernel”. This kernel uses the MXR algorithm, fusing it with all the other five GDN kernels, and supporting chunk size 128. This yields a final speedup of $2.5\times$ compared to the baseline.

6 Conclusion

In this work we revisited triangular inversion algorithms in the context of Linear Attention with the Delta-Rule. We studied both direct and iterative methods, focusing on algorithms that are rich in matrix products and have the potential to efficiently utilize modern hardware that supports such operations. For each method, a detailed numerical stability and complexity analysis was provided, highlighting their effectiveness and their robustness against numerical errors. Besides the theoretical properties, we provided detailed experimental evaluations, covering a wide-spectrum of properties. These included numerical accuracy benchmarks, both at the kernel-level, in different floating point formats, and at the end-to-end model accuracy level. Moreover, we implemented and empirically evaluated the performance of the methods on NPUs. At the kernel level, our fastest and stable implementation achieved up to $4.3\times$ speedup against optimized baselines, and up to $2.5\times$ speedup at the entire model-layer level, when optimized as a whole. We hope that these findings will serve as a guidance for fast and robust AI kernel development, with high performance, and, importantly, reliable numerical results.

References

- [1] James R. Bunch and John E. Hopcroft. Triangular factorization and inversion by fast matrix multiplication. *Mathematics of Computation*, 28(125):231–236, 1974.
- [2] Rezaul Chowdhury, Francesco Silvestri, and Flavio Vella. A computational model for tensor core units. In *Proceedings of Symposium on Parallelism in Algorithms and Architectures (SPAA)*, pages 519–521, 2020.
- [3] Rezaul Chowdhury, Francesco Silvestri, and Flavio Vella. Algorithm design for tensor units. In *International Conference on Parallel and Distributed Computing (Euro-Par)*, pages 353–367. Springer, 2021.
- [4] Bruno Codenotti, Mauro Leoncini, and Franco P Preparata. The role of arithmetic in fast parallel matrix inversion. *Algorithmica*, 30(4):685–707, 2001.
- [5] Tri Dao and Albert Gu. Transformers are SSMS: generalized models and efficient algorithms through structured state space duality. In *International Conference on Machine Learning (ICML)*, ICML’24. JMLR, 2024.
- [6] James Demmel, Ioana Dumitriu, and Olga Holtz. Fast linear algebra is stable. *Numerische Mathematik*, 108(1):59–91, October 2007.
- [7] Jeremy J. Du Croz and Nicholas J. Higham. Stability of methods for matrix inversion. *IMA Journal of Numerical Analysis*, 12(1):1–19, 1992.
- [8] Efstratios Gallopoulos, Bernard Philippe, and Ahmed H. Sameh. *Parallelism in Matrix Computations*. Springer Netherlands, 2016.
- [9] Gene H. Golub and Charles F. Van Loan. *Matrix Computations - 4th Edition*. Johns Hopkins University Press, Philadelphia, PA, 2013.

- [10] Dan Hendrycks, Collin Burns, Steven Basart, Andy Zou, Mantas Mazeika, Dawn Song, and Jacob Steinhardt. Measuring Massive Multitask Language Understanding. *International Conference on Learning Representations (ICLR)*, 2021.
- [11] Nicholas J. Higham. Iterative refinement for linear systems and LAPACK. *IMA Journal of Numerical Analysis*, 17(4):495–509, 1997.
- [12] Nicholas J. Higham. *Accuracy and Stability of Numerical Algorithms*. Society for Industrial and Applied Mathematics, January 2002.
- [13] Jiaxi Hu, Yongqi Pan, Jusen Du, Disen Lan, Xiaqiang Tang, Qingsong Wen, Yuxuan Liang, and Weigao Sun. Improving bilinear RNN with closed-loop control. In *Advances in Neural Information Processing Systems (NeurIPS)*, 2026.
- [14] Weizhe Hua, Zihang Dai, Hanxiao Liu, and Quoc Le. Transformer quality in linear time. In *International Conference on Machine Learning (ICML)*, pages 9099–9117. PMLR, 2022.
- [15] Su Jianlin. The elements of DeltaNet’s core inverse matrix are always within $[-1, 1]$. Available online: <https://spaces.ac.cn/archives/11563>, Jan 2026.
- [16] Angelos Katharopoulos, Apoorv Vyas, Nikolaos Pappas, and François Fleuret. Transformers are RNNs: Fast Autoregressive Transformers with Linear Attention. In *International Conference on Machine Learning (ICML)*, pages 5156–5165. PMLR, 2020.
- [17] Kimi Team, Yu Zhang, Zongyu Lin, Xingcheng Yao, Jiaxi Hu, Fanqing Meng, Chengyin Liu, Xin Men, Songlin Yang, Zhiyuan Li, Wentao Li, Enzhe Lu, Weizhou Liu, Yanru Chen, Weixin Xu, Longhui Yu, Yejie Wang, Yu Fan, Longguang Zhong, Enming Yuan, Dehao Zhang, Yizhi Zhang, T. Y. Liu, Haiming Wang, Shengjun Fang, Weiran He, Shaowei Liu, Yiwei Li, Jianlin Su, Jiezhong Qiu, Bo Pang, Junjie Yan, Zhejun Jiang, Weixiao Huang, Bohong Yin, Jiacheng You, Chu Wei, Zhengtao Wang, Chao Hong, Yutian Chen, Guanduo Chen, Yucheng Wang, Huabin Zheng, Feng Wang, Yibo Liu, Mengnan Dong, Zheng Zhang, Siyuan Pan, Wenhao Wu, Yuhao Wu, Longyu Guan, Jiawen Tao, Guohong Fu, Xinran Xu, Yuzhi Wang, Guokun Lai, Yuxin Wu, Xinyu Zhou, Zhilin Yang, and Yulun Du. Kimi linear: An expressive, efficient attention architecture, 2025.
- [18] Cleve B Moler. Iterative refinement in floating point. *Journal of the ACM*, 14(2):316–321, 1967.
- [19] Victor Pan and John Reif. Efficient parallel solution of linear systems. In *Proceedings of the Symposium on Theory of Computing (STOC)*, pages 143–152, 1985.
- [20] Victor Pan and Robert Schreiber. An improved newton iteration for the generalized inverse of a matrix, with applications. *SIAM Journal on Scientific and Statistical Computing*, 12(5):1109–1130, 1991.
- [21] Bo Peng, Ruichong Zhang, Daniel Goldstein, Eric Alcaide, Xingjian Du, Haowen Hou, Jiaju Lin, Jiaxing Liu, Janna Lu, William Merrill, Guangyu Song, Kaifeng Tan, Saiteja Utpala, Nathan Wilce, Johan S. Wind, Tianyi Wu, Daniel Wuttke, and Christian Zhou-Zheng. RWKV-7 “Goose” with Expressive Dynamic State Evolution. In *Second Conference on Language Modeling*, 2025.
- [22] Ahmed H. Sameh and Richard P. Brent. Solving triangular systems on a parallel computer. *SIAM Journal on Numerical Analysis*, 14(6):1101–1113, December 1977.
- [23] Imanol Schlag, Kazuki Irie, and Jürgen Schmidhuber. Linear Transformers Are Secretly Fast Weight Programmers. In Marina Meila and Tong Zhang, editors, *International Conference on Machine Learning (ICML)*, volume 139 of *Proceedings of Machine Learning Research*, pages 9355–9366. PMLR, 18–24 Jul 2021.
- [24] Günther Schulz. Iterative berechnung der reziproken matrix. *ZAMM - Journal of Applied Mathematics and Mechanics / Zeitschrift für Angewandte Mathematik und Mechanik*, 13(1):57–59, January 1933.
- [25] SGLang Project Contributors. SGLang-Kernel-NPU: SGLang Kernel Library for Ascend NPU. <https://github.com/sgl-project/sgl-kernel-npu>, 2025. Accessed: 2026-05-06.

- [26] Rikhav Shah. Hermitian diagonalization in linear precision. In *Proceedings of the ACM-SIAM Symposium on Discrete Algorithms (SODA)*, pages 5599–5615. SIAM, 2025.
- [27] Aleksandros Sobczyk, Giuseppe Sorrentino, and Anastasios Zouzias. Segmented Operations using Matrix Multiplications. *arXiv preprint arXiv:2506.23906*, 2025.
- [28] Torsten Söderström and Gilbert W. Stewart. On the Numerical Properties of an Iterative Method for Computing the Moore–Penrose Generalized Inverse. *SIAM Journal on Numerical Analysis*, 11(1):61–74, March 1974.
- [29] TileLang Contributors. TileLang-Ascend: Ascend TileLang Adapter. <https://github.com/tile-ai/tilelang-ascend>, 2025. Accessed: 2026-05-06.
- [30] Ashish Vaswani, Noam Shazeer, Niki Parmar, Jakob Uszkoreit, Llion Jones, Aidan N. Gomez, Lukasz Kaiser, and Illia Polosukhin. Attention is all you need. *Advances in Neural Information Processing Systems (NeurIPS)*, 30, 2017.
- [31] Divakar Viswanath and Lloyd Nicholas Trefethen. Condition numbers of random triangular matrices. *SIAM Journal on Matrix Analysis and Applications*, 19(2):564–581, 1998.
- [32] Lei Wang, Yu Cheng, Yining Shi, Zhiwen Mo, Zhengju Tang, Wenhao Xie, Tong Wu, Lingxiao Ma, Yuqing Xia, Jilong Xue, Fan Yang, and Zhi Yang. TileLang: Bridge Programmability and Performance in Modern Neural Kernels. In *International Conference on Learning Representations (ICLR)*, 2026.
- [33] James H. Wilkinson. *Progress report on the automatic computing engine*. Mathematics Division, Department of Scientific & Industrial Research, 1948.
- [34] James H. Wilkinson. Error analysis of direct methods of matrix inversion. *Journal of the ACM*, 8(3):281–330, 1961.
- [35] Mingyu Xu, Tenglong Ao, Jiaao He, Jianqiao Lu, Guang Shi, and Shu Zhong. DeltaFormer: Unlock the state space of Transformer. In *Advances in Neural Information Processing Systems (NeurIPS)*, 2025.
- [36] Songlin Yang, Jan Kautz, and Ali Hatamizadeh. Gated Delta Networks: Improving Mamba2 with Delta Rule. In Y. Yue, A. Garg, N. Peng, F. Sha, and R. Yu, editors, *International Conference on Learning Representations (ICLR)*, volume 2025, pages 29687–29707, 2025.
- [37] Songlin Yang, Bailin Wang, Yikang Shen, Rameswar Panda, and Yoon Kim. Gated linear attention transformers with hardware-efficient training. In *International Conference on Machine Learning (ICML)*, ICML’24. JMLR, 2024.
- [38] Songlin Yang, Bailin Wang, Yu Zhang, Yikang Shen, and Yoon Kim. Parallelizing linear transformers with the delta rule over sequence length. In A. Globerson, L. Mackey, D. Belgrave, A. Fan, U. Paquet, J. Tomczak, and C. Zhang, editors, *Advances in Neural Information Processing Systems (NeurIPS)*, volume 37, pages 115491–115522. Curran Associates, Inc., 2024.
- [39] Malik Zaka Ullah, Fazlollah Soleymani, and Abdulrahman S. Al-Fhaid. An efficient matrix iteration for computing weighted Moore–Penrose inverse. *Applied Mathematics and Computation*, 226:441–454, January 2014.
- [40] Lianmin Zheng, Liangsheng Yin, Zhiqiang Xie, Chuyue Sun, Jeff Huang, Cody Hao Yu, Shiyi Cao, Christos Kozyrakis, Ion Stoica, Joseph E. Gonzalez, Clark Barrett, and Ying Sheng. SGLang: Efficient execution of structured language model programs. In *Advances in Neural Information Processing Systems (NeurIPS)*, 2024.
- [41] Shu Zhong, Mingyu Xu, Tenglong Ao, and Guang Shi. Understanding transformer from the perspective of associative memory, 2025.
- [42] Anastasios Zouzias and William F. McColl. A parallel scan algorithm in the tensor core unit model. In *International Conference on Parallel and Distributed Computing (Euro-Par)*, pages 489–502, 2023.

A Code availability

The source code for the kernels and the scripts to reproduce the experimental evaluations are available in the following links:

- <https://github.com/huawei-csl/pto-kernels>
- <https://github.com/huawei-csl/gdn-tri-inverse>
- <https://github.com/huawei-csl/megagdn-pto>

B Floating point model

Floating point error analysis becomes more and more important in AI computing, especially with the recent trend of reducing the bits of precision in floating point formats. For the purposes of this note, we recall some basic definitions, and refer to the classic textbook of Higham [12] for further details.

In the standard floating point model, the floating point representation $\mathbf{fl}(x)$ of a real number x is a $(1 + p + t)$ -bit number:

$$\mathbf{fl}(x) = \pm 2^e \times \left(\frac{m_1}{2} + \frac{m_2}{2^2} + \dots + \frac{m_t}{2^t} \right), \quad (8)$$

where one bit stores the sign of the number \pm , p bits are used to store the (integral) exponent e in the so-called “biased” format, and t bits m_1, m_2, \dots, m_t are used for the *significand* (also known as the *mantissa*). For all *normalized* numbers it holds that:

$$\mathbf{fl}(x) = (1 + \theta)x, \quad |\theta| \leq 2^{-t} := \mathbf{u}, \quad (9)$$

where \mathbf{u} is referred to as the *machine precision*. Normalized numbers are all numbers that can be represented within the given exponent range. Given two (normalized) floating point numbers a, b , floating point operations $\circ \in \{+, -, \times, /\}$ and square roots are assumed to satisfy:

$$\mathbf{fl}(a \circ b) = (1 + \theta)(a \circ b), \quad \text{and} \quad \mathbf{fl}(\sqrt{a}) = (1 + \theta)\sqrt{a}. \quad (10)$$

C Deferred proofs

C.1 Proof of Corollary 2.1

Proof. It holds that $\max_{i,j} |\mathbf{A}_{i,j}| \leq 1$, and from [15] we know that $\max_{i,j} |\mathbf{A}_{i,j}^{-1}| \leq 1$. For any matrix \mathbf{M} , it holds that $\|\mathbf{M}\|_2 \leq n \cdot \max_{i,j} |\mathbf{M}_{i,j}|$, which implies that $\|\mathbf{A}\|_2 \leq n$ and $\|\mathbf{A}^{-1}\|_2 \leq n$, and thus $\kappa(\mathbf{A}) = \|\mathbf{A}\|_2 \|\mathbf{A}^{-1}\|_2 \leq n^2$. \square

C.2 Proof of Lemma 3.1

Proof. [22] proved that, for any vector \mathbf{b} , the returned solution $\tilde{\mathbf{x}}$ for the linear system $\mathbf{A}\mathbf{x} = \mathbf{b}$ satisfies $(\mathbf{A} + \mathbf{E})\tilde{\mathbf{x}} = \mathbf{b}$, where $\|\mathbf{E}\|_\infty \leq C \cdot n^2 \log(n) \cdot \kappa^2(\mathbf{A}) \cdot \|\mathbf{A}\|_\infty \cdot \mathbf{u}$. Since we apply the algorithm for every column of the identity as \mathbf{b} , we can [12, Theorem 7.4], which implies that $\|\tilde{\mathbf{A}}^{-1} - \mathbf{A}^{-1}\|_\infty \leq \xi \cdot \|\mathbf{A}^{-1}\|_\infty$, where $\xi := \frac{\|\mathbf{A}^{-1}\|_\infty \|\mathbf{E}\|_\infty}{1 - \|\mathbf{A}^{-1}\|_\infty \|\mathbf{E}\|_\infty}$. Using standard norm inequalities we can finally argue that

$$\begin{aligned} \|\tilde{\mathbf{A}}^{-1} - \mathbf{A}^{-1}\|_2 &\leq \sqrt{n} \|\tilde{\mathbf{A}}^{-1} - \mathbf{A}^{-1}\|_\infty \\ &\leq \frac{\|\mathbf{A}^{-1}\|_\infty \|\mathbf{E}\|_\infty}{1 - \|\mathbf{A}^{-1}\|_\infty \|\mathbf{E}\|_\infty} \cdot \|\mathbf{A}^{-1}\|_\infty \\ &\leq C' \cdot \|\mathbf{A}^{-1}\|_\infty \cdot n^2 \log(n) \cdot \kappa^2(\mathbf{A}) \cdot \|\mathbf{A}\|_\infty \cdot \mathbf{u} \cdot \|\mathbf{A}^{-1}\|_\infty \\ &\leq C' \cdot n^{3.5} \log(n) \cdot \kappa^3(\mathbf{A}) \cdot \mathbf{u} \cdot \|\mathbf{A}^{-1}\|_2, \end{aligned}$$

where the third step requires the assumption that the machine precision is sufficiently small, so that following bound needs to be satisfied: $\|\mathbf{A}^{-1}\|_\infty \|\mathbf{E}\|_\infty \ll 1$. \square

where $\mu(n), \mu''(n)$ are low-degree polynomials in n , $\psi(k, c, d) := \prod_{i=1}^k (1 + (c \cdot \|\mathbf{L}\|_2)^{2^{i+d}})$, and $\phi(k) := \left[\psi(k, 1, 0) \cdot (2\|\mathbf{L}\|_2)^{2^k} + (1 + \|\mathbf{L}\|_2) \cdot 2^{2^k} \cdot \psi(k, 2, 1) \cdot \left(1 + (2\|\mathbf{L}\|_2)^{2^{k+1}}\right) \right]$.

Proof. Let us first bound the errors for the repeated squaring part, which is completely independent from the computation of the inverse. That is, we focus on lines 3 and 4 of Algorithm 5. Before we start the analysis, we state some preliminaries and define notation. Using standard bounds on floating point analysis of matrix multiplication, we assume access to an algorithm that computes a matrix $\tilde{\mathbf{C}}$ that approximates the product \mathbf{A}, \mathbf{B} such that:

$$\|\tilde{\mathbf{C}} - \mathbf{AB}\|_2 \leq \mu(n) \cdot \|\mathbf{A}\|_2 \cdot \|\mathbf{B}\|_2 \cdot \mathbf{u}, \quad (13)$$

where $\mu(n)$ is some low-degree polynomial in n .

We also make the following explicit assumption on \mathbf{u} which is necessary for our analysis to yield the advertised bounds:

$$\mathbf{u} \leq \frac{1}{2^n \cdot \mu(n)}. \quad (14)$$

Now, let us define $\tilde{\mathbf{Y}}_k$ to be the matrix that is being computed numerically at iteration $k = 1, 2, \dots, \log(n/2)$, and let $\mathbf{Y}_k = \mathbf{Y}^{2^k}$ be the true matrix at iteration k if the computation was carried out in infinite precision.

From Eq. (13), $\tilde{\mathbf{Y}}_k$ satisfies:

$$\tilde{\mathbf{Y}}_k = \tilde{\mathbf{Y}}_{k-1}^2 + \mathbf{E}_k^{MM},$$

where \mathbf{E}_k^{MM} is an error matrix that arises due to floating point errors, and it satisfies $\|\mathbf{E}_k^{MM}\|_2 \leq \mu(n) \cdot \|\tilde{\mathbf{Y}}_{k-1}^2\|_2 \cdot \mathbf{u}$.

$$\begin{aligned} \|\tilde{\mathbf{Y}}_k\|_2 &= \|\tilde{\mathbf{Y}}_{k-1}^2 + \mathbf{E}_k^{MM}\|_2 \\ &\leq \|\tilde{\mathbf{Y}}_{k-1}\|_2^2 + \|\mathbf{E}_k^{MM}\|_2 \\ &\leq \|\tilde{\mathbf{Y}}_{k-1}\|_2^2 + \mu(n) \cdot \|\tilde{\mathbf{Y}}_{k-1}^2\|_2 \cdot \mathbf{u} \\ &= \|\tilde{\mathbf{Y}}_{k-1}\|_2^2 \cdot (1 + \mu(n) \cdot \mathbf{u}) \\ &\leq 2 \cdot \|\tilde{\mathbf{Y}}_{k-1}\|_2^2, \end{aligned}$$

where in the last step we used Inequality (14). Recall that for $k = 1$, we have that $\|\tilde{\mathbf{Y}}_1\|_2 \leq \|\mathbf{Y}_0\|_2^2$, where \mathbf{Y}_0 is the initial matrix. Using this as a base case and solving the recursion, it follows that:

$$\|\tilde{\mathbf{Y}}_k\|_2 \leq 2 \cdot 2^2 \cdot 2^4 \cdot \dots \cdot 2^{2^{k-1}} \cdot \|\tilde{\mathbf{Y}}_1\|_2^{2^k} \leq 2^{2^k-1} \cdot \|\mathbf{Y}_0\|_2^{2^{k+1}}. \quad (15)$$

This allows us to directly obtain a bound on the matrix multiplication error at iteration k :

$$\begin{aligned} \|\mathbf{E}_k^{MM}\|_2 &\leq \mu(n) \cdot \|\tilde{\mathbf{Y}}_{k-1}^2\|_2 \cdot \mathbf{u} \\ &\leq \mu(n) \cdot 2^{2^{k-1}-1} \cdot \|\mathbf{Y}_0\|_2^{2^k} \cdot \mathbf{u}. \end{aligned}$$

Now, let $\mathbf{E}_k := \tilde{\mathbf{Y}}_k - \mathbf{Y}_0^{2^k}$ be the total error matrix at iteration k . We can write:

$$\begin{aligned} \mathbf{Y}_0^{2^k} + \mathbf{E}_k &= \tilde{\mathbf{Y}}_{k-1}^2 + \mathbf{E}_k^{MM} \\ &= (\mathbf{Y}_0^{2^{k-1}} + \mathbf{E}_{k-1})^2 + \mathbf{E}_k^{MM} \\ &= \mathbf{Y}_0^{2^k} + \mathbf{Y}_0^{2^{k-1}} \mathbf{E}_{k-1} + \mathbf{E}_{k-1} \mathbf{Y}_0^{2^{k-1}} + \mathbf{E}_{k-1}^2 + \mathbf{E}_k^{MM}. \end{aligned}$$

In the equation above, the terms $\mathbf{Y}_0^{2^k}$ on the left and the right hand side cancel out. If we take norms on both sides, we can write that:

$$\|\mathbf{E}_k\|_2 \leq 2 \cdot \|\mathbf{Y}_0^{2^{k-1}}\|_2 \cdot \|\mathbf{E}_{k-1}\|_2 + \|\mathbf{E}_{k-1}\|_2^2 + \|\mathbf{E}_k^{MM}\|_2 \quad (16)$$

$$\leq 2 \cdot \|\mathbf{Y}_0\|_2^{2^{k-1}} \cdot \|\mathbf{E}_{k-1}\|_2 + \|\mathbf{E}_{k-1}\|_2^2 + \mu(n) \cdot 2^{2^{k-1}-1} \cdot \|\mathbf{Y}_0\|_2^{2^k} \cdot \mathbf{u}. \quad (17)$$

We will now prove that $\|\mathbf{E}_k\|_2 \leq 2^{2^k} \cdot \|\mathbf{Y}_0\|_2^{2^k} \cdot \mu(n) \cdot \mathbf{u}$ by induction. For the inductive step, we assume that $\|\mathbf{E}_k\|_2 \leq 2^{2^k} \cdot \|\mathbf{Y}_0\|_2^{2^k} \cdot \mu(n) \cdot \mathbf{u}$. It trivially holds in the base case $k = 1$ from Inequality (13). We now prove that if it holds for k , then it holds also for $k + 1$. Inequality (17) implies that:

$$\begin{aligned}
\|\mathbf{E}_{k+1}\|_2 &\leq 2\|\mathbf{Y}_0\|_2^{2^k} \cdot \|\mathbf{E}_k\|_2 + \|\mathbf{E}_k\|_2^2 + 2^{2^k-1} \cdot \|\mathbf{Y}_0\|_2^{2^{k+1}} \cdot \mu(n) \cdot \mathbf{u} \\
&\leq 2\|\mathbf{Y}_0\|_2^{2^k} \cdot 2^{2^k} \|\mathbf{Y}_0\|_2^{2^k} \mu(n) \cdot \mathbf{u} + (2^{2^k} \|\mathbf{Y}_0\|_2^{2^k} \mu(n) \cdot \mathbf{u})^2 + \mu(n) \cdot 2^{2^k-1} \|\mathbf{Y}_0\|_2^{2^{k+1}} \cdot \mathbf{u} \\
&= \|\mathbf{Y}_0\|_2^{2^{k+1}} \cdot \mu(n) \cdot \mathbf{u} \cdot (2 \cdot 2^{2^k} + 2^{2^{k+1}} \cdot \mu(n) \cdot \mathbf{u} + 2^{2^k-1}) \\
&\leq \|\mathbf{Y}_0\|_2^{2^{k+1}} \cdot \mu(n) \cdot \mathbf{u} \cdot (2 \cdot 2^{2^k} + 2^{2^k} + 2^{2^k-1}) \quad (\text{due to Ineq. 14}) \\
&= \frac{7}{2} \cdot 2^{2^k} \cdot \|\mathbf{Y}_0\|_2^{2^{k+1}} \cdot \mu(n) \cdot \mathbf{u} \\
&\leq 2^{2^{k+1}} \cdot \|\mathbf{Y}_0\|_2^{2^{k+1}} \cdot \mu(n) \cdot \mathbf{u},
\end{aligned}$$

where the last holds for all $k \geq 2$.

Next, we shift the attention to the computation of the final \mathbf{X} which approximates the inverse. Let $\tilde{\mathbf{X}}_k$ be the matrix computed at iteration $k \in \{1, \dots, \log(n/2)\}$ in Algorithm 5, line 5, given by the formula $\tilde{\mathbf{X}}_k \leftarrow \tilde{\mathbf{X}}_{k-1} + \tilde{\mathbf{X}}_{k-1} \cdot \tilde{\mathbf{Y}}_k$, where $\tilde{\mathbf{X}}_0 := \mathbf{I} - \mathbf{L}$.

We recall that for the element-wise floating point addition between two matrices \mathbf{A} and \mathbf{B} the returned matrix $\tilde{\mathbf{C}} = \mathbf{fl}(\mathbf{A} + \mathbf{B})$ satisfies:

$$\|\tilde{\mathbf{C}} - (\mathbf{A} + \mathbf{B})\|_2 \leq \mathbf{u} \cdot \sqrt{n} \cdot \|\mathbf{A} + \mathbf{B}\|_2. \quad (18)$$

Using this we can calculate a bound on the error of $\tilde{\mathbf{X}}_k$:

$$\tilde{\mathbf{X}}_k = \tilde{\mathbf{X}}_{k-1} + \tilde{\mathbf{X}}_{k-1} \cdot \tilde{\mathbf{Y}}_k + \mathbf{F}_k^{GEMM},$$

where \mathbf{F}_k^{GEMM} denotes the total error of the ‘‘GEMM’’ operation $\tilde{\mathbf{X}}_{k-1} + \tilde{\mathbf{X}}_{k-1} \cdot \tilde{\mathbf{Y}}_k$. Let $\tilde{\mathbf{Z}}_k := \mathbf{fl}(\tilde{\mathbf{X}}_{k-1} \cdot \tilde{\mathbf{Y}}_k) = \tilde{\mathbf{X}}_{k-1} \cdot \tilde{\mathbf{Y}}_k + \mathbf{F}_k^{MM}$, where \mathbf{F}_k^{MM} is the error of the multiplication $\tilde{\mathbf{X}}_{k-1} \cdot \tilde{\mathbf{Y}}_k$. It satisfies $\|\mathbf{F}_k^{MM}\| \leq \mu(n) \cdot \mathbf{u} \cdot \|\tilde{\mathbf{X}}_{k-1}\|_2 \cdot \|\tilde{\mathbf{Y}}_k\|_2$, which implies that $\|\tilde{\mathbf{Z}}_k\|_2 \leq \|\tilde{\mathbf{X}}_{k-1}\|_2 \cdot \|\tilde{\mathbf{Y}}_k\|_2 \cdot (1 + \mu(n) \cdot \mathbf{u})$. For the subsequent addition, we have that:

$$\begin{aligned}
\mathbf{fl}(\tilde{\mathbf{X}}_{k-1} + \tilde{\mathbf{Z}}_k) &:= \tilde{\mathbf{X}}_{k-1} + \tilde{\mathbf{Z}}_k + \mathbf{F}_k^{ADD} \\
&= \tilde{\mathbf{X}}_{k-1} + \tilde{\mathbf{X}}_{k-1} \cdot \tilde{\mathbf{Y}}_k + \mathbf{F}_k^{MM} + \mathbf{F}_k^{ADD},
\end{aligned}$$

where, from Inequality (18), it holds that:

$$\begin{aligned}
\|\mathbf{F}_k^{ADD}\|_2 &\leq \mathbf{u} \cdot \sqrt{n} \cdot \|\tilde{\mathbf{X}}_{k-1} + \tilde{\mathbf{Z}}_k\|_2 \\
&\leq \mathbf{u} \cdot \sqrt{n} \cdot \left(\|\tilde{\mathbf{X}}_{k-1}\|_2 + \|\tilde{\mathbf{X}}_{k-1}\|_2 \cdot \|\tilde{\mathbf{Y}}_k\|_2 \cdot (1 + \mu(n) \cdot \mathbf{u}) \right) \\
&= \mathbf{u} \cdot \sqrt{n} \cdot \|\tilde{\mathbf{X}}_{k-1}\|_2 \cdot \left(1 + \|\tilde{\mathbf{Y}}_k\|_2 \cdot (1 + \mu(n) \cdot \mathbf{u}) \right).
\end{aligned}$$

This finally gives:

$$\begin{aligned}
\|\mathbf{F}_k^{GEMM}\|_2 &= \|\mathbf{F}_k^{ADD} + \mathbf{F}_k^{MM}\|_2 \\
&\leq \mu(n) \cdot \mathbf{u} \cdot \|\tilde{\mathbf{X}}_{k-1}\|_2 \cdot \|\tilde{\mathbf{Y}}_k\|_2 + \mathbf{u} \cdot \sqrt{n} \cdot \|\tilde{\mathbf{X}}_{k-1}\|_2 \cdot \left(1 + \|\tilde{\mathbf{Y}}_k\|_2 \cdot (1 + \mu(n) \cdot \mathbf{u}) \right) \\
&\leq \mu'(n) \cdot \mathbf{u} \cdot \|\tilde{\mathbf{X}}_{k-1}\|_2 \cdot \left(1 + \|\tilde{\mathbf{Y}}_k\|_2 \cdot (2 + \mu(n) \cdot \mathbf{u}) \right) \\
&\leq \mu'(n) \cdot \mathbf{u} \cdot \|\tilde{\mathbf{X}}_{k-1}\|_2 \cdot \left(1 + 2^{2^k-1} \cdot \|\mathbf{Y}_0\|_2^{2^{k+1}} \cdot (2 + \mu(n) \cdot \mathbf{u}) \right) \\
&\leq \mu'(n) \cdot \mathbf{u} \cdot \|\tilde{\mathbf{X}}_{k-1}\|_2 \cdot \left(1 + 2^{2^{k+1}} \cdot \|\mathbf{Y}_0\|_2^{2^{k+1}} \right),
\end{aligned}$$

where $\mu'(n)$ (similar to $\mu(n)$) is polynomial in n . We can get a bound on $\|\tilde{\mathbf{X}}_k\|_2$ in a similar way that we did with $\|\tilde{\mathbf{Y}}_k\|_2$. We have that:

$$\begin{aligned}
\|\tilde{\mathbf{X}}_k\|_2 &= \|\tilde{\mathbf{X}}_{k-1} + \tilde{\mathbf{X}}_{k-1}\tilde{\mathbf{Y}}_k + \mathbf{F}_k^{GEMM}\|_2 \\
&\leq \|\tilde{\mathbf{X}}_{k-1}\|_2 \cdot \left(1 + \|\tilde{\mathbf{Y}}_k\|_2 + \mu'(n) \cdot \mathbf{u} \cdot \left(1 + 2^{2^k+1} \cdot \|\mathbf{Y}_0\|_2^{2^{k+1}}\right)\right) \\
&\leq \|\tilde{\mathbf{X}}_{k-1}\|_2 \cdot \left(1 + 2^{2^k+1} \cdot \|\mathbf{Y}_0\|_2^{2^{k+1}}\right) \cdot (1 + \mu'(n) \cdot \mathbf{u}) \\
&\leq 2 \cdot \|\tilde{\mathbf{X}}_{k-1}\|_2 \cdot \left(1 + 2^{2^k+1} \cdot \|\mathbf{Y}_0\|_2^{2^{k+1}}\right) \\
&\leq \|\mathbf{X}_0\|_2 \cdot 2^{2^k} \cdot \prod_{i=1}^k \left(1 + 2^{2^i+1} \cdot \|\mathbf{Y}_0\|_2^{2^{i+1}}\right) \\
&\leq \|\mathbf{X}_0\|_2 \cdot 2^{2^k} \cdot \prod_{i=1}^k \left(1 + (2 \cdot \|\mathbf{Y}_0\|_2)^{2^{i+1}}\right) \tag{19}
\end{aligned}$$

$$\leq (1 + \|\mathbf{Y}_0\|_2) \cdot 2^{2^k} \cdot \prod_{i=1}^k \left(1 + (2 \cdot \|\mathbf{Y}_0\|_2)^{2^{i+1}}\right). \tag{20}$$

Finally, we can consider the final error of the algorithm. Let us write $\tilde{\mathbf{X}}_k = \mathbf{X}_k + \mathbf{F}_k$, where now \mathbf{F}_k contains all the errors of the final returned matrix. By using the same methodology as before with \mathbf{Y}_k and \mathbf{E}_k , for all $k = 1, \dots, \log(n/2)$ we can write:

$$\begin{aligned}
\mathbf{X}_k + \mathbf{F}_k &= (\mathbf{X}_{k-1} + \mathbf{F}_{k-1}) + (\mathbf{X}_{k-1} + \mathbf{F}_{k-1})(\mathbf{Y}_k + \mathbf{E}_k) + \mathbf{F}_k^{GEMM} \\
&= \mathbf{X}_{k-1} + \mathbf{F}_{k-1} + \mathbf{X}_{k-1}\mathbf{Y}_k + \mathbf{X}_{k-1}\mathbf{E}_k + \mathbf{F}_{k-1}\mathbf{Y}_k + \mathbf{F}_{k-1}\mathbf{E}_k + \mathbf{F}_k^{GEMM},
\end{aligned}$$

where $\mathbf{F}_0 = 0$. This gives:

$$\begin{aligned}
\mathbf{F}_k &= \mathbf{F}_{k-1} + \mathbf{X}_{k-1}\mathbf{E}_k + \mathbf{F}_{k-1}\mathbf{Y}_k + \mathbf{F}_k^{GEMM} \\
&= \mathbf{F}_{k-1}(\mathbf{I} + \mathbf{Y}_k + \mathbf{E}_k) + \mathbf{X}_{k-1}\mathbf{E}_k + \mathbf{F}_k^{GEMM} \\
&= \mathbf{F}_{k-1}(\mathbf{I} + \mathbf{Y}_k + \mathbf{E}_k) + \mathbf{X}_{k-1}\mathbf{E}_k + \mathbf{F}_k^{GEMM}. \tag{21}
\end{aligned}$$

Let us denote $a(k) := \|\mathbf{I} + \mathbf{Y}_k + \mathbf{E}_k\|_2$ and $\beta(k) := \|\mathbf{X}_{k-1}\mathbf{E}_k + \mathbf{F}_k^{GEMM}\|_2$. By taking the norm of \mathbf{F}_k we arrive to a first-order linear recurrence:

$$\|\mathbf{F}_k\|_2 \leq \|\mathbf{F}_{k-1}\|_2 \cdot a(k) + \beta(k) \leq \beta(k) + \sum_{j=1}^{k-1} \beta(j) \cdot \prod_{i=j+1}^k a(i) \tag{22}$$

Let us now bound the terms $a(k)$ and $\beta(k)$. We have that:

$$\begin{aligned}
a(k) &= \|\mathbf{I} + \mathbf{Y}_k + \mathbf{E}_k\|_2 \\
&\leq \left(1 + \|\mathbf{Y}_0\|_2^{2^k} + 2^{2^k} \cdot \|\mathbf{Y}_0\|_2^{2^k} \cdot \mu(n) \cdot \mathbf{u}\right) \\
&\leq 1 + 2\|\mathbf{Y}_0\|_2^{2^k}.
\end{aligned}$$

Let $\psi(k, c, d) := \prod_{i=1}^k (1 + (c \cdot \|\mathbf{Y}_0\|_2)^{2^{i+d}})$. The products of $a(k)$'s can be bounded as:

$$\prod_{i=1}^k a(i) \leq \prod_{i=1}^k (1 + 2\|\mathbf{Y}_0\|_2^{2^i}) \leq \prod_{i=1}^k (1 + (2 \cdot \|\mathbf{Y}_0\|_2)^{2^i}) = \psi(k, 2, 0).$$

For $\beta(k)$, we have that:

$$\begin{aligned}
\beta(k) &= \|\mathbf{X}_{k-1}\mathbf{E}_k + \mathbf{F}_k^{GEMM}\|_2 \\
&\leq \|\mathbf{X}_{k-1}\|_2 \cdot \|\mathbf{E}_k\|_2 + \|\mathbf{F}_k^{GEMM}\|_2 \\
&\leq \|\mathbf{X}_{k-1}\|_2 \cdot 2^{2^k} \cdot \|\mathbf{Y}_0\|_2^{2^k} \cdot \mu(n) \cdot \mathbf{u} + \mu'(n) \cdot \mathbf{u} \cdot \|\tilde{\mathbf{X}}_{k-1}\|_2 \cdot \left(1 + 2^{2^k+1} \cdot \|\mathbf{Y}_0\|_2^{2^{k+1}}\right) \\
&\leq \mu''(n) \cdot \mathbf{u} \cdot \left[\|\mathbf{X}_{k-1}\|_2 \cdot 2^{2^k} \cdot \|\mathbf{Y}_0\|_2^{2^k} + \|\tilde{\mathbf{X}}_{k-1}\|_2 \cdot \left(1 + 2^{2^k+1} \cdot \|\mathbf{Y}_0\|_2^{2^{k+1}}\right)\right], \tag{23}
\end{aligned}$$

where $\mu''(n) = \max(\mu(n), \mu'(n))$. To proceed further, we bound:

$$\begin{aligned}
\|\mathbf{X}_{k-1}\|_2 &= \|\mathbf{X}_{k-1} + \mathbf{X}_{k-1}\mathbf{Y}_k\|_2 \\
&\leq \|\mathbf{X}_{k-1}\| \cdot \|\mathbf{I} + \mathbf{Y}_k\|_2 \\
&\leq \|\mathbf{X}_{k-1}\| \cdot (1 + \|\mathbf{Y}_0\|_2^{2^k}) \\
&\leq \prod_{i=1}^k (1 + \|\mathbf{Y}_0\|_2^{2^i}) \\
&= \psi(k, 1, 0).
\end{aligned} \tag{24}$$

Combining Inequalities (20), (23), and (24), we obtain:

$$\begin{aligned}
\beta(k) &\leq \mu''(n) \cdot \mathbf{u} \cdot \left[\|\mathbf{X}_{k-1}\|_2 \cdot 2^{2^k} \cdot \|\mathbf{Y}_0\|_2^{2^k} + \|\tilde{\mathbf{X}}_{k-1}\|_2 \cdot \left(1 + 2^{2^k+1} \cdot \|\mathbf{Y}_0\|_2^{2^{k+1}}\right) \right] \\
&\leq \mu''(n) \cdot \mathbf{u} \cdot \left[\psi(k, 1, 0) \cdot (2\|\mathbf{Y}_0\|_2)^{2^k} + (1 + \|\mathbf{Y}_0\|_2) \cdot 2^{2^k} \cdot \psi(k, 2, 1) \cdot \left(1 + (2\|\mathbf{Y}_0\|_2)^{2^{k+1}}\right) \right] \\
&= \mu''(n) \cdot \mathbf{u} \cdot \phi(k),
\end{aligned} \tag{25}$$

where $\phi(k) := \left[\psi(k, 1, 0) \cdot (2\|\mathbf{Y}_0\|_2)^{2^k} + (1 + \|\mathbf{Y}_0\|_2) \cdot 2^{2^k} \cdot \psi(k, 2, 1) \cdot \left(1 + (2\|\mathbf{Y}_0\|_2)^{2^{k+1}}\right) \right]$. Then the main error of Inequality (22) becomes:

$$\|\mathbf{F}_k\|_2 \leq \mu''(n) \cdot \mathbf{u} \cdot \left(\phi(k) + \sum_{j=1}^{k-1} \phi(j) \cdot \frac{\psi(k, 2, 0)}{\psi(j, 2, 0)} \right). \tag{26}$$

□

D Additional experiments and implementation details

D.1 Parallelization and asynchronous execution

To achieve the best possible performance, we highlight some high-level practices. First, note that, in existing implementations of linear transformers architectures, the triangular inversion part is inherently massively parallel. Typically, the input is given as a high-dimensional tensor with numerous small-sized chunks, which are all completely independent, and can be inverted without communication. However, internally, within the inversion algorithms, there are data dependencies between each iteration (or recursion level, for the recursive ones). The effect of these dependencies can be mitigated to a minimal level by pipelining.

As an example, in the repeated-squaring algorithm (MCH), Step 1. depends on the corresponding \mathbf{Y} matrix from the previous iteration, while Step 2. expects as an input the output of Step 1. However, the update of \mathbf{Y} in iteration $k + 1$ is independent of the update of $\tilde{\mathbf{X}}$ in iteration k , and therefore these two operations can be overlapped, if enough matrix cores are available. Similar observations can be made for the other algorithms as well. At the ‘‘I/O level’’, since individual chunks are independent, it is possible to overlap the inversion of a chunk while simultaneously loading the next chunk from the main (slow) memory to the local memory.

D.2 Stability analysis on different types of matrices

Here we add some additional experiments regarding the numerical accuracy of the methods on different classes of matrices. In Figure 6 we provide the same experiment as in Figure 2, where the strictly lower-triangular part of the input matrix is additionally scaled by a decay factor. As expected, this scaling benefits the accuracy of all algorithms. MXR, in particular, gains 1 or 2 digits of precision for each data-type and matrix size.

D.3 MMLU Benchmarks

Massive Multitask Language Understanding (MMLU) [10] is a widely used benchmark for evaluating large language models. It consists of thousands of multiple-choice questions spanning 57 subjects. In

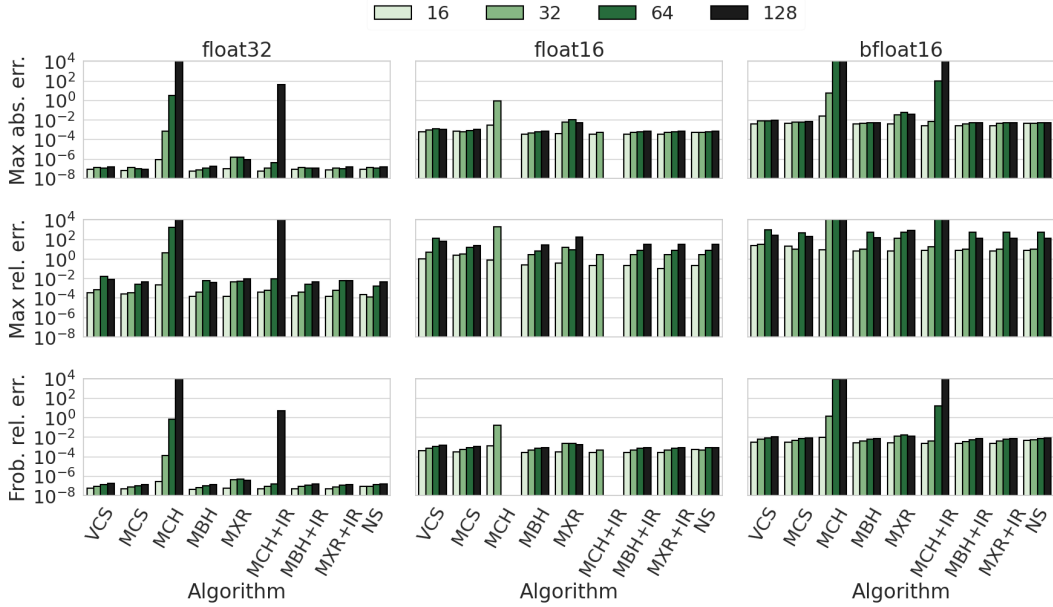


Figure 6: Comparison of the inverse accuracy of various methods, for three different input precision formats, and four matrix sizes.

this work, we use only a subset of these subjects to speed up evaluation. This is justified because our goal is not to assess the absolute capabilities of a model, but rather to perform a relative comparison that highlights how algorithmic accuracy affects end-to-end performance.

Figure 7 illustrates the average accuracy obtained on the MMLU benchmark, for 10 different subjects, for three different models with different inverse algorithms. All algorithms in Figure 7 are on-par with the baseline accuracy. This figure complements Figure 2, which already show-cased that the unstable algorithm MCH can lead to catastrophic accuracy drop, when used naively.

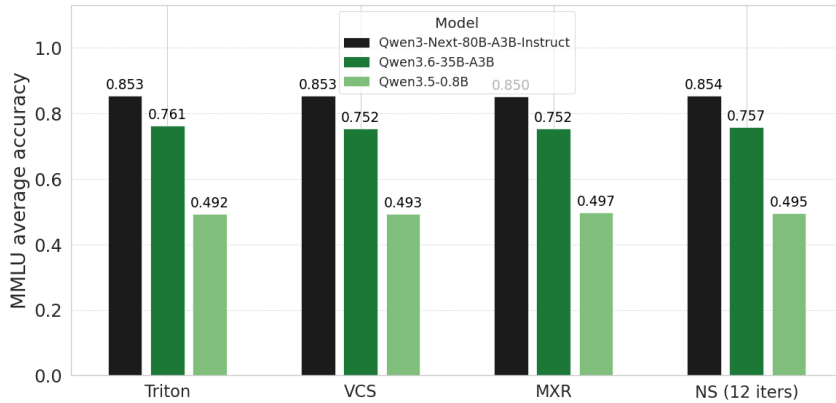


Figure 7: Comparison of the accuracy obtained on MMLU (10-subjects) of different models with different inverse algorithms.

In Tab. 3 and 4 we report the full results of the MMLU benchmarks summarized in Fig. 7 and Fig. 3 respectively:

Table 3: MMLU accuracy (10-subject subset) across inversion methods and Qwen models.

Model	Method	Avg.	AbsAlg	Anatomy	Astron	BusEth	ClinKn	ColBio	ColChem	ColCS	ColMath	ColMed
Qwen3-80B-A3B	Triton	0.853	0.800	0.807	0.934	0.810	0.894	0.972	0.670	0.850	0.780	0.861
	VCS	0.853	0.800	0.815	0.934	0.810	0.894	0.972	0.670	0.840	0.770	0.867
	MXR	0.850	0.800	0.800	0.934	0.800	0.894	0.965	0.670	0.850	0.760	0.861
	NS-12	0.854	0.800	0.807	0.941	0.810	0.891	0.972	0.680	0.860	0.770	0.861
Qwen3-35B-A3B	Triton	0.761	0.480	0.830	0.737	0.850	0.823	0.944	0.470	0.770	0.680	0.803
	VCS	0.752	0.460	0.830	0.737	0.830	0.811	0.931	0.460	0.760	0.700	0.780
	MXR	0.752	0.500	0.830	0.717	0.830	0.819	0.951	0.440	0.750	0.680	0.775
	NS-12	0.757	0.460	0.837	0.743	0.840	0.826	0.938	0.450	0.790	0.680	0.775
Qwen3.5-0.8B	Triton	0.492	0.320	0.467	0.500	0.510	0.581	0.618	0.470	0.420	0.350	0.491
	VCS	0.493	0.330	0.467	0.507	0.500	0.581	0.604	0.490	0.420	0.330	0.503
	MXR	0.497	0.330	0.452	0.507	0.540	0.600	0.590	0.490	0.440	0.310	0.503
	NS-12	0.495	0.330	0.467	0.493	0.530	0.589	0.604	0.490	0.430	0.330	0.491

Table 4: MMLU accuracy (10-subject subset) across Newton-Schulz iteration counts and Qwen models.

Model	Method	Avg.	AbsAlg	Anatomy	Astron	BusEth	ClinKn	ColBio	ColChem	ColCS	ColMath	ColMed
Qwen3-80B-A3B	NS-2	0.082	0.130	0.044	0.059	0.130	0.060	0.076	0.030	0.060	0.130	0.127
	NS-4	0.289	0.250	0.400	0.263	0.270	0.302	0.410	0.110	0.290	0.240	0.272
	NS-6	0.816	0.680	0.807	0.941	0.820	0.864	0.938	0.640	0.770	0.680	0.821
	NS-8	0.847	0.780	0.815	0.934	0.820	0.883	0.965	0.670	0.850	0.760	0.850
	NS-10	0.854	0.800	0.807	0.941	0.810	0.891	0.965	0.670	0.860	0.780	0.867
	NS-12	0.854	0.800	0.807	0.941	0.810	0.891	0.972	0.680	0.860	0.770	0.861
	NS-14	0.852	0.800	0.807	0.934	0.810	0.891	0.965	0.670	0.850	0.780	0.861
Qwen3-35B-A3B	NS-2	0.025	0.000	0.104	0.013	0.030	0.019	0.014	0.020	0.000	0.000	0.035
	NS-4	0.045	0.130	0.074	0.092	0.000	0.030	0.014	0.010	0.000	0.000	0.075
	NS-6	0.708	0.360	0.733	0.868	0.750	0.770	0.882	0.460	0.710	0.530	0.728
	NS-8	0.710	0.410	0.704	0.737	0.830	0.766	0.917	0.420	0.790	0.610	0.717
	NS-10	0.757	0.480	0.837	0.750	0.830	0.823	0.944	0.460	0.760	0.660	0.792
	NS-12	0.757	0.460	0.837	0.743	0.840	0.826	0.938	0.450	0.790	0.680	0.775
Qwen3.5-0.8B	NS-2	0.000	0.000	0.000	0.000	0.000	0.000	0.000	0.000	0.000	0.000	0.000
	NS-4	0.182	0.170	0.333	0.211	0.170	0.155	0.236	0.080	0.170	0.030	0.202
	NS-6	0.329	0.260	0.363	0.375	0.320	0.377	0.354	0.250	0.330	0.230	0.312
	NS-8	0.500	0.320	0.467	0.507	0.550	0.600	0.576	0.480	0.410	0.350	0.526
	NS-10	0.490	0.320	0.474	0.487	0.510	0.574	0.611	0.490	0.420	0.340	0.491
	NS-12	0.495	0.330	0.467	0.493	0.530	0.589	0.604	0.490	0.430	0.330	0.491
NS-14	0.484	0.310	0.452	0.487	0.500	0.577	0.604	0.490	0.410	0.320	0.486	